JOURNAL OF VIROLOGY, Dec. 2002, p. 12149–12161 Vol. 76, No. 23
0022-538X/02/$04.00+0 DOI: 10.1128/JVI.76.23.12149–12161.2002

Noninvasive Bioluminescence Imaging of Herpes Simplex Virus Type 1 Infection and Therapy in Living Mice

Gary D. Luker,[1,2] J. Patrick Bardill,[3] Julie L. Prior,[1,2] Christina M. Pica,[1,2] David Piwnica-Worms,[1,2] and David A. Leib[3,4]*

Molecular Imaging Center, Mallinckrodt Institute of Radiology,[1] and Departments of Molecular Biology and Pharmacology,[2] Molecular Microbiology,[3] and Ophthalmology and Visual Sciences,[4] Washington University School of Medicine, St. Louis, Missouri 63110

Received 6 June 2002/Accepted 26 August 2002

Mouse models of herpes simplex virus type 1 (HSV-1) infection provide significant insights into viral and host genes that regulate disease pathogenesis, but conventional methods to determine the full extent of viral spread and replication typically require the sacrifice of infected animals. To develop a noninvasive method for detecting HSV-1 in living mice, we used a strain KOS HSV-1 recombinant that expresses firefly (*Photinus pyralis*) and *Renilla* (*Renilla reniformis*) luciferase reporter proteins and monitored infection with a cooled charge-coupled device camera. Viral infection in mouse footpads, peritoneal cavity, brain, and eyes could be detected by bioluminescence imaging of firefly luciferase. The activity of *Renilla* luciferase could be imaged after direct administration of substrate to infected eyes but not following the systemic delivery of substrate. The magnitude of bioluminescence from firefly luciferase measured in vivo correlated directly with input titers of recombinant virus used for infection. Treatment of infected mice with valacyclovir, a potent inhibitor of HSV-1 replication, produced dose-dependent decreases in firefly luciferase activity that correlated with changes in viral titers. These data demonstrate that bioluminescence imaging can be used for noninvasive, real-time monitoring of HSV-1 infection and therapy in living mice.

Herpes simplex virus type 1 (HSV-1) is a widespread human pathogen that infects ca. 80% of all persons by adulthood (33). During acute infection, HSV-1 enters the body at epithelial and mucosal surfaces, where viral replication and subsequent lysis of epithelial cells and fibroblasts lead to infection of sensory neurons and intraaxonal transport of virus to neuronal cell bodies in sensory ganglia. Further viral replication occurs within ganglia, and HSV-1 may reemerge from the nervous system during acute infection and cause disease by zosteriform spread within the same dermatome as the initial site of infection (3, 9, 15). Ultimately, viral gene expression in sensory ganglia is repressed and nonproductive latent infection is established (23). In response to poorly defined stimuli, HSV-1 may reactivate from latency and produce new infectious virus. Both primary infection with HSV-1 and reactivation from latency can cause morbidity and some mortality from diseases such as blinding keratitis and encephalitis.

Studies of HSV-1 in mouse models typically rely upon observations of cutaneous manifestations of disease, cultures from accessible epithelial surfaces, and sacrifice of infected mice to determine distribution and titer of virus. Although these experimental methods have allowed investigators to define viral and host genes that regulate replication and virulence of HSV-1 in vivo (10, 18, 19, 24, 30), these assay techniques preclude real-time monitoring of the kinetics and extent of disease progression in the same animal. Therefore, potentially significant insights from animal-to-animal variations in host-pathogen relationships may be missed with conventional protocols for determining viral infection and therapeutic response. Spread of HSV-1 to unexpected anatomic sites also may not be identified because the infected tissue is not assayed for virus. Thus, noninvasive, whole-body imaging of HSV-1 infection in living mice could provide new insights into disease pathogenesis and treatment.

Recent advances in biotechnology have enabled in vivo imaging of luciferase reporter proteins in living mice by using a cooled charge-coupled device (CCD) camera (6, 34). Because bioluminescence imaging has minimal background activity, this technology is very sensitive for detecting light emitted from luciferases. As little as 38 pg of firefly (*Photinus pyralis*) luciferase (FL) per g of liver tissue has been detected with bioluminescence imaging in vivo (20). D-Luciferin, the substrate for FL, crosses cell membranes and penetrates the intact blood-brain barrier after intraperitoneal (i.p.) injection in mice, allowing this reporter protein to be imaged in any anatomic site. At the concentrations used for bioluminescence imaging, D-luciferin is nontoxic and nonimmunogenic, so serial imaging examinations can be performed with the same mouse. Using region-of-interest (ROI) analysis of images to quantify light emission, bioluminescence measured in vivo correlates highly with FL activity in lysates of extracted tissues (26, 34). Although light is attenuated and scattered by hair and other overlying tissues (5), bioluminescence imaging has been used to detect and localize FL in tumor xenografts and parenchymal organs, including lung, liver, and brain tissues (1, 26, 34). Bacterial infections also have been detected in vivo with this imaging modality by using bacteria expressing the *lux* operon (11, 12).

In addition to FL and bacterial luciferase, a recently pub-

* Corresponding author. Mailing address: Department of Ophthalmology and Visual Sciences, Washington University School of Medicine, Box 8096, 660 S. Euclid Ave., St. Louis, MO 63110. Phone: (314) 362-2689. Fax: (314) 362-3638. E-mail: Leib@vision.wustl.edu.

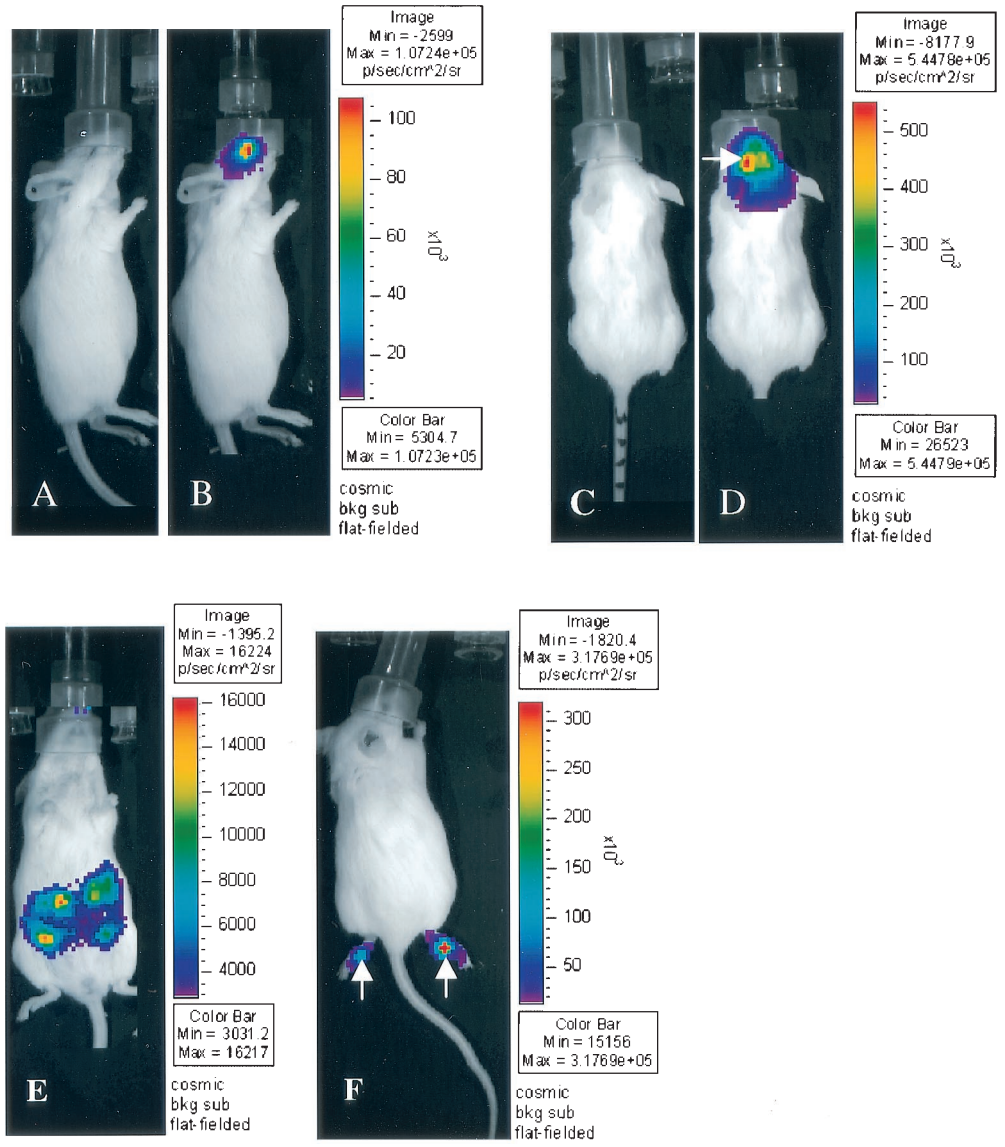

FIG. 1. Bioluminescence imaging of FL in mice infected with KOS/Dlux/oriL by the corneal-scarification (A and B), i.c. (C and D), i.p. (E), or footpad (F) routes of inoculation ($n = 2$ for each site). Mice were infected with 2×10^4 (C and D) or 2×10^6 (A, B, E, and F) PFU of KOS/Dlux/oriL virus, and bioluminescence imaging of FL was performed 3 days later. Representative images obtained from a 5-min acquisition are shown for each site of infection (B, D, E, and F). The pseudocolor scale shows relative photon flux on each image. Note that the minimum and maximum values for photon flux differ among the images. Panels A and C depict gray-scale photographs obtained immediately before bioluminescence imaging of mice in panels B and D. The white arrows in panels D and F shows foci of increased bioluminescence that correspond to the needle track for i.c. and footpad injections of KOS/Dlux/oriL, respectively.

lished study has demonstrated the feasibility of imaging luciferase from *Renilla reniformis* (RL) at various anatomic sites in living mice (2). FL and RL each have unique substrates and show distinct kinetics of light production in vivo. RL activity peaks within 1 min and is undetectable by ca. 10 min after intravenous injection of the cognate RL substrate coelenterazine, whereas light from FL is maximal at 3 to 4 min and declines slowly over 30 min. Therefore, FL and RL potentially could be used as reporters for imaging two different molecular events in vivo.

In the present study, we determined the feasibility of using bioluminescence imaging to monitor infection with HSV-1 in living mice. We used a recombinant HSV-1 strain KOS virus (KOS/Dlux/oriL) that expresses FL and RL from early gene promoters (27). Replication and spread of KOS/Dlux/oriL in the mouse ocular model of infection does not differ significantly from wild-type strain KOS, making this reporter virus an effective model for studying pathogenesis of HSV-1. FL activity from KOS/Dlux/oriL was detected by bioluminescence imaging at all tested sites of infection. Although bioluminescence from RL also could be imaged in the ocular model of infection, our results indicate that pharmacokinetics and bioavailability of substrate may limit applications of this reporter protein for in vivo imaging of HSV-1. Using ROI analysis of photon emis-

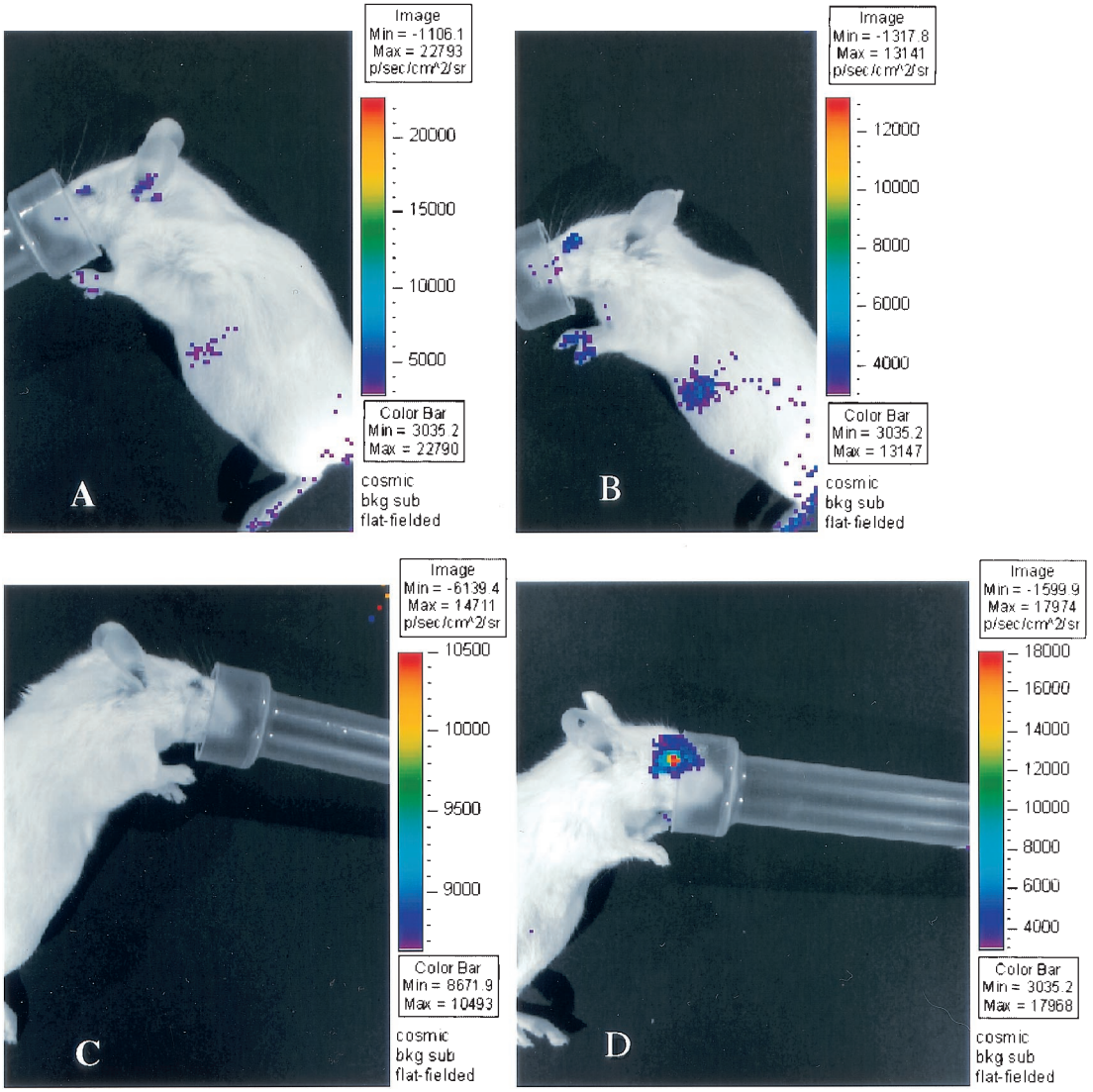

FIG. 2. Bioluminescence imaging of RL in the mouse ocular model of infection. Mice were mock infected (A and C) or infected with 2×10^6 PFU of KOS/Dlux/oriL (B and D) by corneal scarification. Bioluminescence imaging of RL was performed after tail vein injection of 4 μg of coelenterazine (A and B)/ml or direct administration of coelenterazine (2 μg/ml in 10 μl) to the surface of each eye (C and D). Images are representative of two mock-infected and three infected mice each for tail vein or eye delivery of coelenterazine.

sion, we demonstrate that differences in viral titer can be quantified by bioluminescence imaging of FL, allowing real-time imaging of disease progression and response to therapy.

MATERIALS AND METHODS

Recombinant viruses. KOS/Dlux/oriL was constructed by homologous recombination into a site between UL49 and UL50 with a cassette encoding the divergent UL29 and UL30 promoters and oriL region regulating firefly and *Renilla* luciferases (27). The oriL- and promoter-containing fragment was a 435-bp *Bam*HI-*Sma*I fragment comprising HSV-1 nucleotide positions 62238 to 62673. Viral stocks were propagated on Vero cells (25).

Animal procedures. All animal procedures were approved by the Washington University School of Medicine Animal Studies Committee. Outbred CD-1 female mice (body weight, 20 to 25 g; Charles River Breeding Laboratories, Inc., Kingston, N.Y.) were inoculated with KOS/Dlux/oriL or wild-type KOS at various anatomic sites: (i) intracranial (i.c.), 2×10^4 PFU in a 20-μl volume (16); (ii) footpad, 2×10^6 PFU in 50-μl volume; (iii), i.p., 2×10^6 PFU in a 100-μl volume; and (iv) ocular, various titers as indicated in figure legends in a 5-μl volume administered by corneal scarification as described previously (25). Mice were anesthetized with ketamine and xylazine before i.c., footpad, and ocular injections of virus, whereas i.p. injections were performed without anesthesia. For i.c. infection, mice were injected in the left cerebral hemisphere to a depth of 3 mm. The injection site was equidistant from the outer canthus of the eye, front of the pinna, and midline of the skull. Mock infections at various anatomic sites were performed in an identical fashion, except that no virus was used.

To monitor the effect of valacyclovir on ocular infection with KOS/Dlux/oriL, treatment was begun by adding either 0.1 or 1 mg of valacyclovir (GlaxoSmithKline, Collegeville, Pa.)/ml to drinking water after bioluminescence imaging on day 1 postinoculation. Mice were allowed to consume drug-containing water ad libitum, and water was changed daily throughout the time course of therapy to maintain a fresh preparation of valacyclovir. Tear film material was assayed daily for virus following bioluminescence imaging as described previously (25). Before bioluminescence imaging on days 1 and 5 of the time course experiments, the heads of each animal were shaved to decrease attenuation and scattering of transmitted light by hair.

Bioluminescence imaging. Imaging of FL in mice was performed by i.p. injection of 150 μg of D-luciferin (Xenogen Corp., Alameda, Calif.)/g from a 15-mg/ml stock solution in phosphate-buffered saline. Approximately 5 min after injection, animals were anesthetized with metofane, and imaging began 10 min

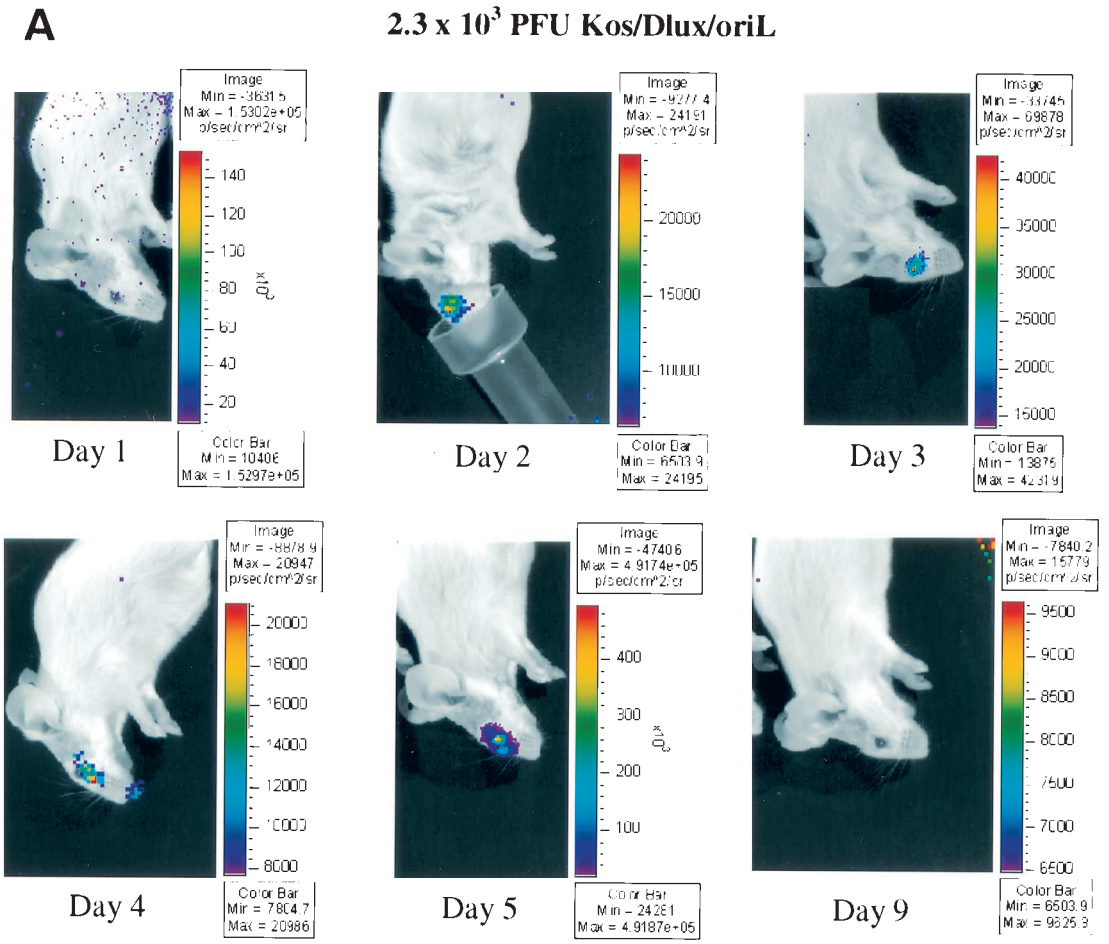

FIG. 3. Time course of infection with increasing initial titers of KOS/Dlux/oriL in living mice. Mice ($n = 2$ for each group) were infected by corneal scarification with ca. 2×10^2 to 2×10^6 PFU of virus, and the progression of infection was monitored by bioluminescence imaging and the titers of KOS/Dlux/oriL from tear film material on days 1 to 5 and day 9 postinfection. Representative images of mice infected with 2.3×10^3 (A) and 1.2×10^6 (B) PFU are shown. The minimum and maximum values for photon flux differ among images in order to use the full dynamic range of the pseudocolor scale for each examination. Mean values for photon flux (C) and viral titers from tear film material (D) on each day are presented. The lower limits of detection for viral titers are 10 PFU. (E) AUC analyses for photon flux (black bars) and viral titers (open bars) over the course of the experiment are presented for each group of mice. Note the log scale for graphs in panels D and E. Error bars in these and subsequent figures represent the standard error + or ± the SEM for the bar graphs or line graphs, respectively.

after administration of D-luciferin. Stock solutions of coelenterazine (Biotium, Hayward, Calif.), a substrate for RL, were prepared at a concentration of 2 mg/ml in methanol (2) or ethanol for tail vein or ocular administration, respectively. Further dilutions were made in 50 mM sodium phosphate buffer for tail vein injection (2) or 150 mM sodium chloride for ocular delivery of substrate, respectively. Mice were anesthetized with metofane and imaged immediately after tail vein injection of 4 μg of coelenterazine/g or ocular administration of 2 μg of coelenterazine/ml in a 10-μl volume. Anesthesia was maintained during imaging by nose cone delivery of metofane as necessary.

Bioluminescence imaging of luciferase was performed on the xenogen in vivo imaging system (IVIS), which consists of a cooled CCD camera mounted on a light-tight specimen chamber, cryogenic refrigeration unit, camera controller, and a computer system for data analysis. We initially acquired a gray-scale surface image of each mouse by using a 10-cm field-of-view, a 0.2-s exposure time, a binning (resolution) factor of 2, a 16 f/stop (aperture), and an open filter. Immediately afterward, imaging of in vivo bioluminescence was performed with animals positioned to place various anatomic sites of interest toward the CCD camera. Animal positioning was based on the site of viral inoculation. Bioluminescence images were obtained for acquisition times of 1, 2, or 5 min, depending on amounts of light produced at various sites of infection. Bioluminescence imaging was performed with a binning factor of 4 for time course experiments or a binning factor of 8 for other studies, a 1 f/stop, and an open filter.

Quantification of bioluminescence data. Relative intensities of transmitted light from in vivo bioluminescence were represented as a pseudocolor image ranging from violet (least intense) to red (most intense). Corresponding gray-scale photographs and color luciferase images were superimposed with LivingImage (Xenogen) and Igor (Wavemetrics, Lake Oswego, Oreg.) image analysis software. Signal intensities from ROIs were defined manually, and data were expressed as photon flux (photons/s/cm^2/steradian), where steradian (sr) refers to the photons emitted from a unit solid angle of a sphere. Background photon flux was defined from an ROI of the same size drawn over the thorax of each animal, and these data were subtracted from signal intensities measured at sites of infection. Area-under-the-curve (AUC) analyses were performed with Kaleidagraph (Synergy Software, Reading, Pa.). Data were reported as mean values ± the standard error of the mean (SEM) for the number of animals indicated in figure legends. Pairs were compared with Student t test (13), and values of $P \leq 0.05$ were considered significant.

RESULTS

Bioluminescence imaging of reporter virus at various anatomic sites. We recently described a recombinant strain KOS virus (KOS/Dlux/oriL) that expresses both FL and RL reporter

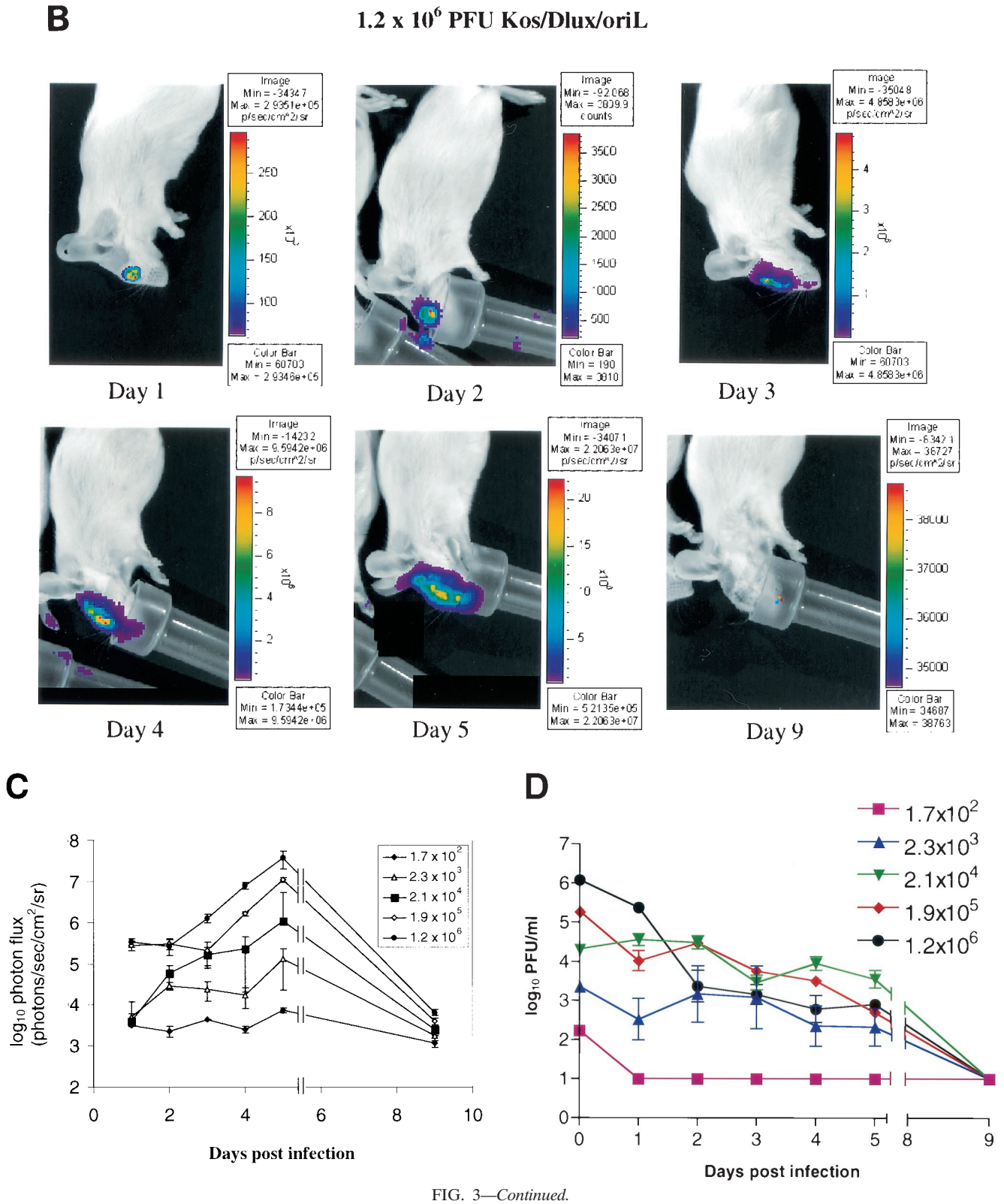

FIG. 3—*Continued.*

proteins from the divergent UL29 and UL30 promoters and oriL region (27). Growth kinetics of KOS/Dlux/oriL are essentially the same as wild-type KOS, and luciferase activity in tissue homogenates increases in proportion to viral replication. Thus, recombinant KOS/Dlux/oriL is established as a valid reporter virus for infection of mice with wild-type KOS.

To determine the feasibility of detecting HSV-1 in vivo with bioluminescence imaging, we inoculated CD-1 mice with KOS/

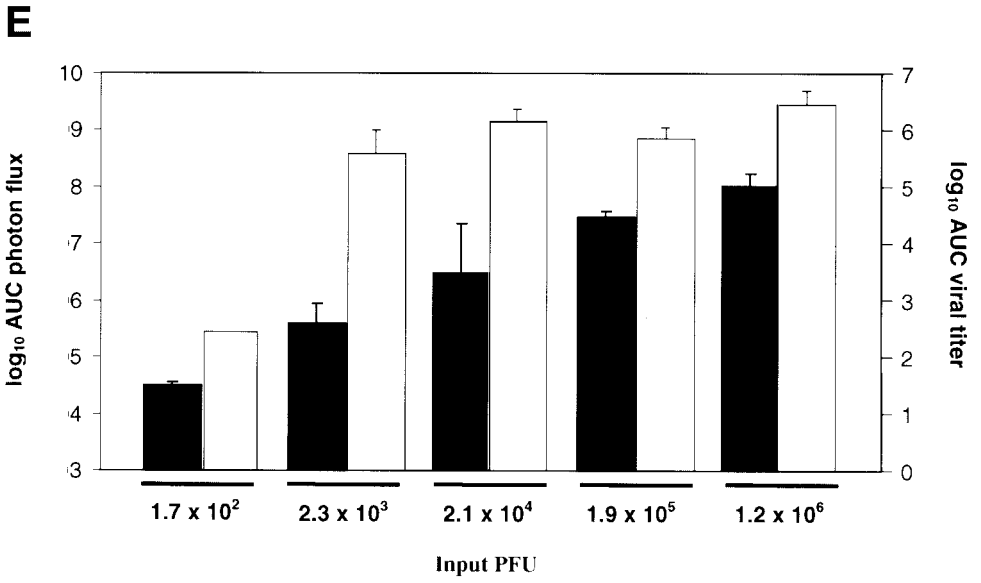

FIG. 3—*Continued.*

Dlux/oriL in four ways: via the footpad (FP) or by i.p., i.c., and corneal routes. Mice received 2×10^4 PFU for i.c. infection and 2×10^6 PFU at all other sites. Animals infected with wild-type KOS were used as controls. Bioluminescence imaging of FL activity in living mice was performed 3 days postinfection. At 10 min after i.p. injection of D-luciferin, 1- and 5-min images of light emission from anesthetized mice were obtained on the IVIS system. The FL activity was detected at all sites of inoculation, although the total photon flux varied among the different routes of infection (Fig. 1). The i.p. infection produced the lowest emission of light, whereas bioluminescence from i.c. infection was the greatest. Foci of increased bioluminescence are seen in the left cerebral hemisphere and in the feet, corresponding to the i.c. and the footpad injection sites, respectively. No bioluminescence could be detected above background levels in mice infected with wild-type KOS (data not shown). These data qualitatively demonstrate that FL produced by infection with recombinant HSV-1 KOS/Dlux/oriL can be imaged in vivo.

Light produced by RL is blue-shifted relative to FL (21), resulting in lower transmission through tissues from photons produced by RL. Nevertheless, bioluminescence imaging of RL in various anatomic sites has been described recently (2). To determine whether imaging of RL can be used to detect infection with KOS/Dlux/oriL in footpads, we initially administered 0.7 μg of coelenterazine/g i.p., a dose and route of substrate delivery that are reported to be sufficient for the in vivo detection of RL (2). We began imaging immediately after injection of coelenterazine and imaged intermittently through 30 min to coincide with the reported rapid onset and diminution of in vivo bioluminescence from RL. However, we were unable to detect activity of RL above background in footpads ($n = 4$), despite the presence of acute viral infection as determined by bioluminescence imaging of FL (data not shown).

Because our previous research with KOS/Dlux/oriL in mice showed that the activity of FL and RL both are readily detectable in tissue homogenates, we postulated that imaging of RL in vivo was limited by bioavailability of substrate to footpads. To test this hypothesis, we increased the dose of coelenterazine to 4 μg/g and administered the substrate by tail vein injection to avoid any potential problems with absorption from the peritoneum. However, light emission from RL remained undetectable above background in footpads infected with KOS/Dlux/oriL (data not shown). We also used ocular infection with KOS/Dlux/oriL to test the bioluminescence imaging of RL in a different anatomic site. No significant difference in ocular bioluminescence from RL could be detected between mice infected with KOS/Dlux/oriL ($n = 3$) and mock-infected controls ($n = 2$) (Fig. 2A and B), although we again documented acute infection with KOS/Dlux/oriL via imaging of FL (data not shown). We then administered coelenterazine directly to eyes of infected ($n = 3$) and mock-infected ($n = 2$) mice on day 5 postinfection with a dose (2 μg/ml in 10 μl) that is effective for detecting RL in cultured cells (2). After topical delivery of the substrate, photon flux was ca. 10-fold greater in the eyes of mice infected with KOS/Dlux/oriL compared with mock-infected controls (Fig. 2C and D). Although these data demonstrate that ocular infection with recombinant HSV-1 KOS/Dlux/oriL can be detected with RL in vivo, imaging of RL in this model system is limited by bioavailability of coelenterazine administered systemically.

Correlation of bioluminescence imaging data with viral titers. Previous studies have demonstrated that light emission in vivo correlates with relative numbers of mammalian cells stably transfected with FL (29) or CFU of bacteria expressing the *lux* operon (12). In vivo measurements of bioluminescence also are correlated highly with light emission measured by in vitro assays of homogenized tissues (34). Because activity of FL in tissue homogenates is proportional to titers of KOS/Dlux/oriL in mice (27), we hypothesized that bioluminescence imaging could be used for real-time, noninvasive monitoring of viral proliferation and distribution during the course of infection. Currently, assays of viral titers from cultures of tear film ma-

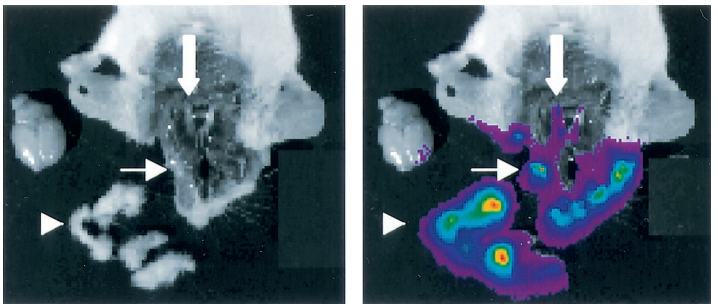

FIG. 4. In situ localization of FL activity 5 days postinfection with 2×10^6 PFU of KOS/Dlux/oriL by corneal scarification. D-Luciferin was injected into living mice ($n = 2$), and animals were sacrificed ca. 15 min after the administration of substrate. (A and B) Representative gray-scale photograph (A) and 2-min bioluminescence image (B) show the distribution of FL activity in the specimen. Arrowhead marks dissected periocular tissues, thin white arrow denotes an eye, and the thick white arrow shows trigeminal ganglia.

terial are the only validated, nonlethal method for monitoring the serial progression of infection in the mouse ocular model.

We used corneal scarification and infection with increasing titers of KOS/Dlux/oriL (from $\sim 2 \times 10^2$ to $\sim 2 \times 10^6$ PFU/eye) to correlate bioluminescent signals with viral titers. Imaging of FL and cultures of tear film material were performed daily from days 1 to 5 and then on day 9 postinfection. Bioluminescence images showed a greater spread of FL activity in mice infected with higher doses of virus (Fig. 3A and B and data not shown). As determined by ROI analysis, photon flux correlated highly with input titers of virus at all time points (Fig. 3C). The FL activity for each inoculum of virus peaked at 5 days postinfection, although this was the only time point at which bioluminescence was significantly above the background level in mice infected with 2×10^2 PFU/eye. By day 9 postinfection, signal from FL in all groups of mice was at or close to background levels for the IVIS system.

At an input dose of 2×10^2 PFU per eye, virus was undetectable in cultures of tear film material obtained at all time points (Fig. 3D). In comparison, FL activity in this group of mice could be imaged above background levels on day 5. Readily detectable titers of virus were obtained from eye swabs on days 1 to 5 postinfection in mice infected with 2×10^3 PFU per eye. Input doses of $2 \times 10^4 - 2 \times 10^6$ PFU per eye all produced titers on day 1 postinfection that were higher than those quantified in animals inoculated with 2×10^3 PFU per eye. As shown previously (17), viral titers subsequently declined in mice inoculated with 2×10^4 to 2×10^6 PFU and generally were comparable among the 2.3×10^3, 2.1×10^4, 1.9×10^5, and 1.2×10^6 PFU cohorts of mice on days 2 to 5 postinfection. No virus could be detected by day 9 postinfection, independent of the input dose of KOS/Dlux/oriL.

To further compare data for bioluminescence and viral replication, we performed area under the curve (AUC) analyses of photon flux and viral titers from tear film material over days 1 to 9 postinfection (Fig. 3E). Data for photon flux showed that increasing input titers of KOS/Dlux/oriL produced stepwise increases in bioluminescence ($P < 0.05$, except $P < 0.09$ for differences between the 2.1×10^4 group and 2.3×10^3 or 1.9×10^5 groups, respectively). Although AUC for viral titers over the course of infection was less in animals infected with 2×10^2 PFU ($P < 0.01$), the AUC did not differ significantly among mice infected with $2 \times 10^3 - 2 \times 10^6$ PFU per eye ($P < 0.2$). Therefore, the data for patterns and the time course of infection are discordant between ROI analysis of photon flux and the viral titers from eye swabs. Given that peak photon flux from bioluminescence imaging coincides with the time of maximum FL activity and the viral titer reported previously in periocular skin, most of the signal measured in the ROI analysis likely originates from periocular skin rather than the cornea (28). HSV-1 enters the periocular skin by zosteriform spread from the innervating ganglia that are seeded from the original infection in the cornea. Nonetheless, these data demonstrate that bioluminescence imaging can be used to monitor the course of infection and differentiate relative differences in titers of HSV-1 in living mice.

To further analyze anatomic localization of FL at the time of peak activity, we injected D-luciferin into mice on day 5 of infection with 2×10^6 PFU of KOS/Dlux/oriL. After the expression of FL in the living animals was confirmed by imaging, we sacrificed each mouse and rapidly performed a limited dissection of soft tissues of the head and i.c. contents. Bioluminescence imaging showed that activity of FL was greatest in the periocular tissues and skin overlying the dorsum of the head (Fig. 4, arrowhead), which demonstrates the extensive zosteriform spread of HSV-1 during infection. However, FL activity from KOS/Dlux/oriL also was observed in eyes (Fig. 4, thin arrow) and trigeminal ganglia (Fig. 4, thick arrow), but no bioluminescence was detected in the brain.

Real-time monitoring of antiviral therapy. Nucleoside analogs such as acyclovir and its orally administered prodrug valacyclovir inhibit HSV-1 DNA polymerase after activation by viral thymidine kinase. These drugs are effective in treating infections with HSV-1 in both mouse models and human patients. To determine whether bioluminescence imaging can monitor efficacy of antiviral therapy in real time, we infected mice with 2×10^6 PFU of recombinant KOS/Dlux/oriL by corneal scarification. Mice were imaged 1 day postinfection, and then animals were left untreated or were treated with 0.1 or 1 mg of valacyclovir/ml in drinking water, respectively. Based on previous studies, these concentrations of drug were anticipated to be within the therapeutic range for inhibiting HSV-1 infection (31).

To monitor the effects of valacyclovir on replication of KOS/Dlux/oriL, bioluminescence imaging was performed on days 1 to 5 and day 9 postinfection and compared with the daily viral titers cultured from tear film material after each imaging study.

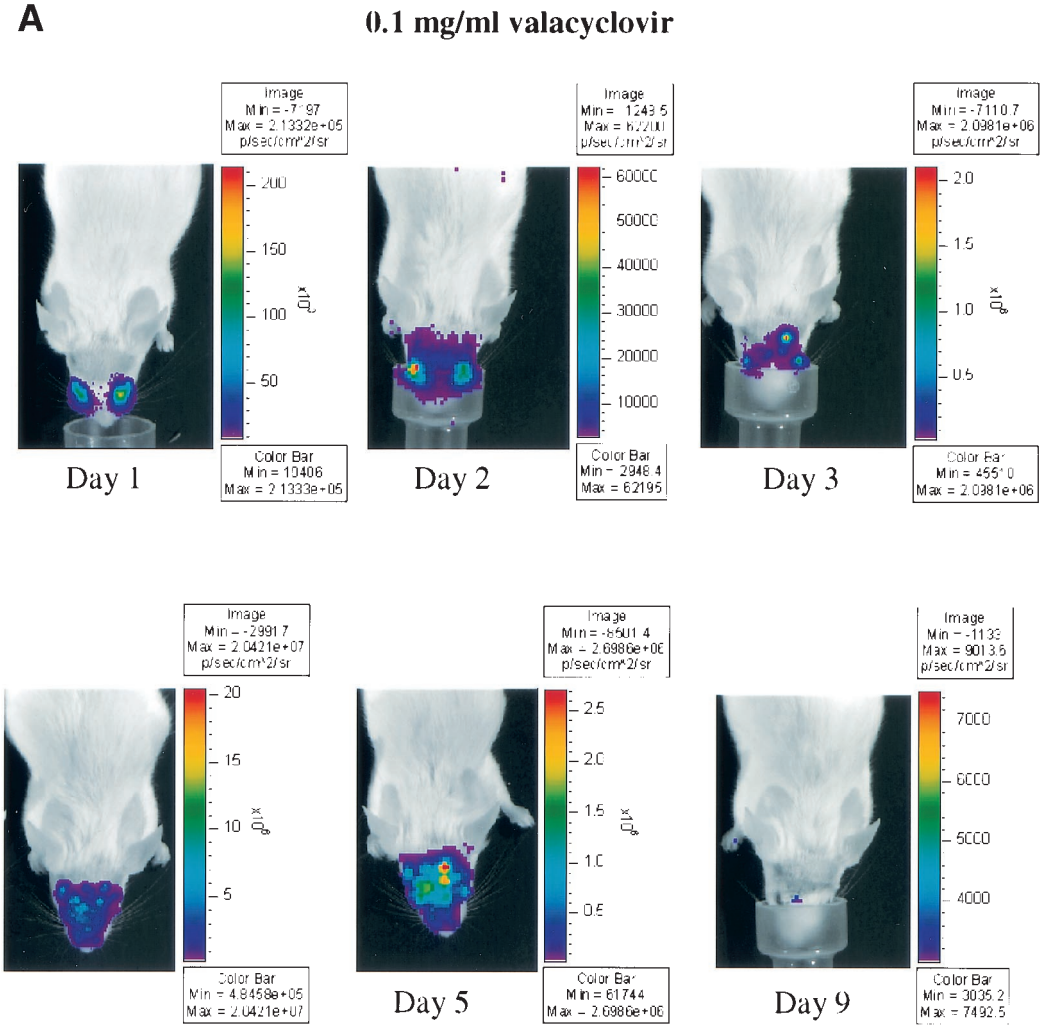

FIG. 5. Time course of KOS/Dlux/oriL infection in response to treatment with valacyclovir. Mice were infected with 2×10^6 PFU KOS/Dlux/oriL by corneal scarification, and treatment with valacyclovir at 0.1 mg/ml ($n = 4$), 1 mg/ml ($n = 4$), or vehicle control ($n = 5$) in drinking water was started after imaging on day 1 day postinfection. Sequential bioluminescence images and eye swabs for tear film material were obtained on days 1 to 5 and 9 of infection. Representative images of mice in the 0.1-mg/ml valacyclovir (A), 1-mg/ml valacyclovir (B), and control groups (C) are presented. The mean ROI values for photon flux (D) and viral titers (E) in each group are shown. The arrow denotes the start of valacyclovir treatment after imaging and culturing tear films on day 1 postinfection. (F) AUC analyses for photon flux (black bars) and viral titers from tear films (open bars) for each cohort of mice.

Qualitative analysis of images showed similar spread of virus from eyes to periocular tissues on the dorsum of the head during days 1 to 4 postinfection in control mice and both treatment groups (Fig. 5A to C). However, the degree of bioluminescence on day 5 was less extensive over periocular tissues in mice treated with 1 mg of valacyclovir/ml. Light emission from KOS/Dlux/oriL typically returned almost to background levels on day 9. However, a low level of bioluminescence infrequently could be detected on day 9, demonstrating biologic variation in response to infection among different mice (Fig. 5C). ROI analysis showed that photon flux after 2 days of treatment (day 3 postinfection) was significantly lower in the 1-mg/ml valacyclovir treatment group than either the 0.1-mg/ml group ($P < 0.025$) or the untreated controls ($P < 0.001$) (Fig. 5D). These differences in photon flux also were observed on days 4 and 5 of infection. In control mice and animals treated with 0.1 mg of valacyclovir/ml, maximum photon flux occurred on day 5 postinfection and subsequently declined. Mice treated with 0.1 mg of valacyclovir/ml had lower FL activity from KOS/Dlux/oriL than control animals on days 3 to 5, although the differences at these individual time points were not statistically significant.

Direct measurements of viral titers from tear film material also showed dose-dependent reductions in response to valacyclovir (Fig. 5E). Titers of KOS/Dlux/oriL decreased in all groups of mice after initiating treatment on day 1 postinfection. In mice receiving 1 mg of valacyclovir/ml, viral titers were significantly less than the 0.1 mg of valacyclovir/ml and control groups on days 2 to 5 postinfection ($P < 0.001$). Treatment with 0.1 mg of valacyclovir/ml also produced titers of KOS/Dlux/oriL that were lower than control on days 2 to 5 postinfection, and these differences were statistically significant on

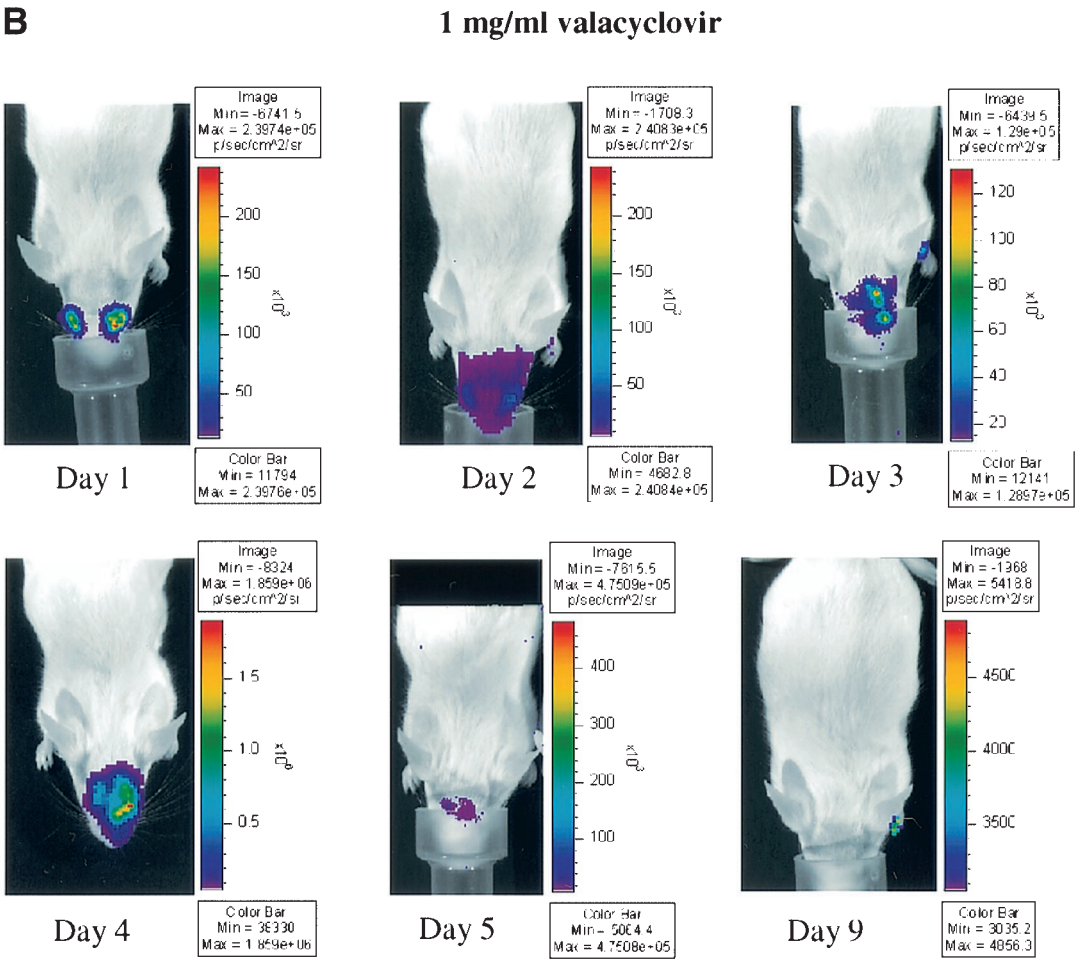

FIG. 5—*Continued.*

days 2 to 4 postinfection ($P < 0.05$). Independent of treatment with valacyclovir, viral titers were undetectable on day 9.

Bioluminescence imaging and viral titers both differentiated among valacyclovir treatment groups and control mice, although the kinetics of response to therapy differed with each measurement technique. Light emission increased through days 4 to 5 postinfection in all mice, but treatment with valacyclovir attenuated bioluminescence in a dose-dependent fashion (Fig. 5D). By comparison, administration of valacyclovir accelerated the decrease in titers of KOS/Dlux/oriL between days 1 to 2 postinfection (Fig. 5E). Differences between data from bioluminescence imaging and viral titers likely reflect the established progression of HSV-1 after ocular infection and the sites quantified with each method. Maximal titers of HSV-1 in eyes are present 1 day after infection and subsequently decline, which is demonstrated by data for titers of KOS/Dlux/oriL in tear film material. As shown in Fig. 3 and 4, most of the bioluminescence quantified by imaging appears to originate from KOS/Dlux/oriL in periocular tissues. Because the amounts of virus in periocular tissues peak at ca. 3 to 4 days postinfection after zosteriform spread from trigeminal ganglia (28), therapeutic effects of valacyclovir are not detected by bioluminescence imaging until later in the course of infection. Nevertheless, both viral titers and imaging data show similar dose-dependent inhibition of KOS/Dlux/oriL by valacyclovir in living mice.

To further characterize overall effects of valacyclovir, we performed AUC analyses of data from bioluminescence imaging and viral titers. Treatment with 1 mg of valacyclovir/ml reduced total photon flux from KOS/Dlux/oriL to ca. 3% of that measured in untreated mice, which is significantly less than both the 0.1-mg/ml valacyclovir and the control groups ($P < 0.025$ and $P < 0.001$, respectively) (Fig. 5F). AUC for FL activity in animals receiving 0.1 mg of valacyclovir/ml was 56% of the value quantified in controls, although differences between the low-dose treatment group and untreated animals did not reach statistical significance ($P < 0.07$). By comparison, AUC data for viral titers from tear film material showed differences among treatment groups and control animals that were slightly greater than bioluminescence imaging (Fig. 5F). In mice treated with 1 mg of valacyclovir/ml, the AUC for viral titers was significantly less than both the 0.1-mg/ml valacyclovir ($P < 0.005$) and control ($P < 0.001$) groups. The 0.1-mg/ml cohort of mice also had significantly lower AUC for virus than control animals ($P < 0.01$). Nevertheless, AUC data for both bioluminescence imaging and viral titers showed similar pat-

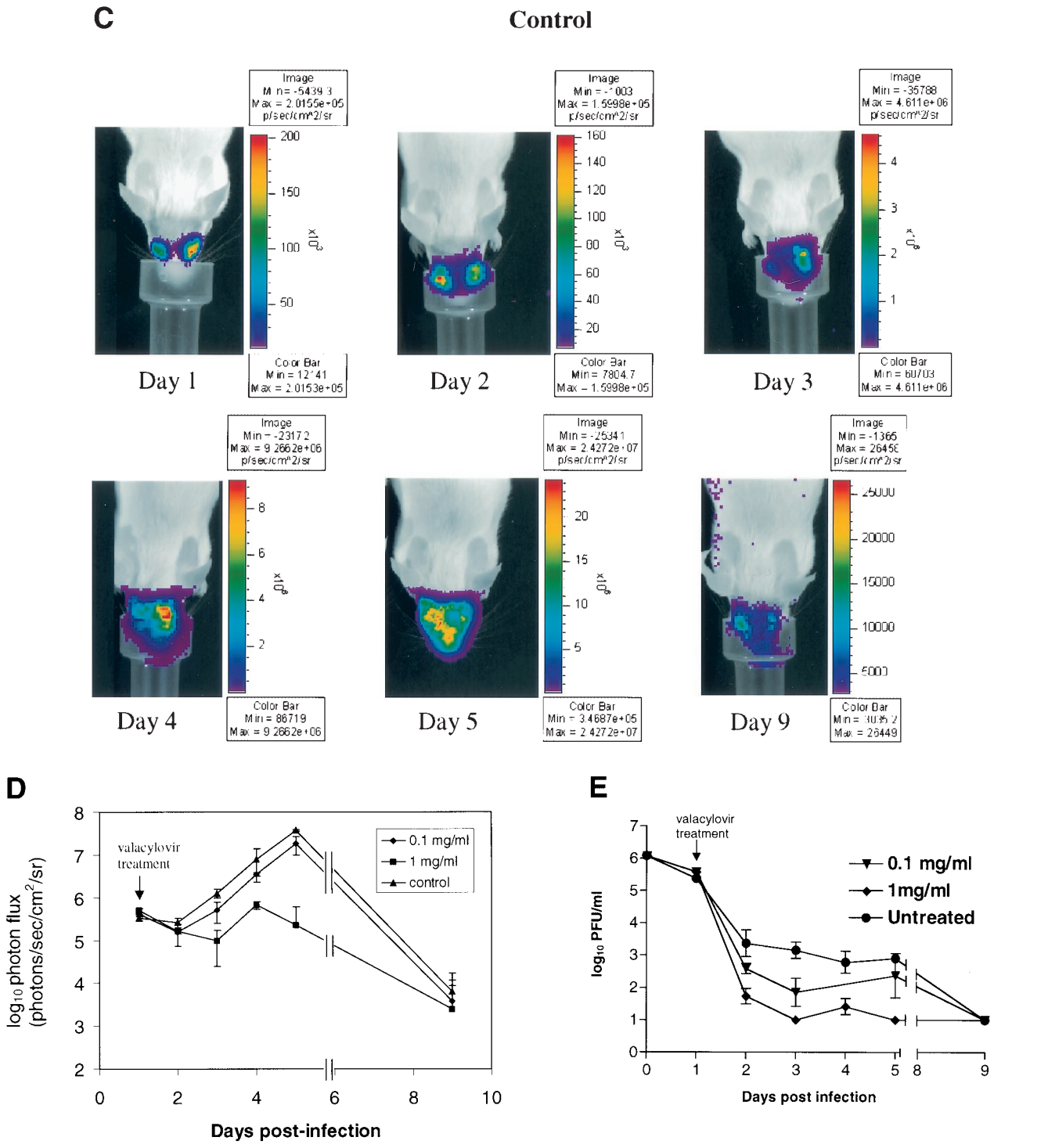

FIG. 5—*Continued.*

terns of response to treatment. We previously established that activity of FL in tissue homogenates corresponds with titers of KOS/Dlux/oriL in living mice, and other investigators have shown a high correlation between in vivo and in vitro measurements of FL in tissues (26, 34). Therefore, these data show that changes in photon flux from bioluminescence imaging can be used to monitor therapy of HSV-1 in intact mice and quantify relative differences in therapeutic efficacy.

DISCUSSION

Mutant HSV-1 viruses have been identified that grow normally in cell culture models but are attenuated significantly in

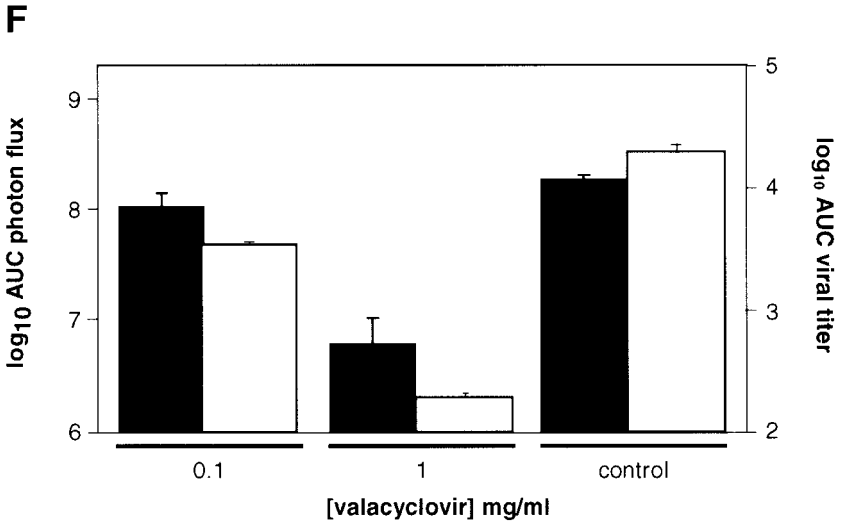

FIG. 5—*Continued.*

vivo (4, 18, 24, 32, 35). Thus, mouse models are essential for defining genes that regulate replication and virulence of HSV-1 during acute and latent stages of infection. However, conventional studies of HSV-1 in mouse models often are limited by the need to sacrifice animals to quantify viral titers, assay reporter gene activity, and determine the full extent of viral spread. Development and application of noninvasive imaging techniques for tracking HSV-1 in living animals would facilitate studies of viral and host genes that regulate viral pathogenesis. Our current study validates bioluminescence imaging for real-time monitoring of viral infection and response to therapy in vivo by using a recombinant HSV-1 virus that expresses luciferase reporter proteins. Infection with KOS/Dlux/oriL at multiple anatomic sites, including the central nervous system, could be detected through bioluminescence imaging of FL. We also demonstrated that progression and spread of HSV-1 infection can be monitored noninvasively with serial imaging studies. There are no published reports of immunogenicity of FL in vivo, and expression of FL in liver of immunocompetent mice has been maintained for 1 year after hydrodynamic transfection of plasmid DNA (22). Thus, these data clearly demonstrate the feasibility of using bioluminescence for real-time, repetitive imaging of HSV-1 infection in living mice.

An important conclusion from the current study is that changes in the viral titer correlate with relative differences in photon flux values quantified in vivo. Because of the direct relationship between the amounts of infectious virus and light emission, we used bioluminescence imaging of FL to monitor treatment of HSV-1 with valacyclovir, a nucleoside analog drug used clinically for the treatment of HSV-1 infections. Based on changes in photon flux over the course of infection, we were able to detect and quantify efficacy of two different doses of valacyclovir in comparison with untreated animals. Data for bioluminescence imaging and viral titers obtained from tear film material showed comparable dose-dependent inhibition of HSV-1, although the effects of a low dose of valacyclovir relative to untreated control animals were differentiated more readily with eye swabs. Kinetics for response to therapy differed between imaging and viral titers because ROI analysis predominantly quantified light emission from periocular tissues, whereas titers were obtained only from eyes. Therefore, data from each method are consistent with effects of valacyclovir on the established progression of HSV-1 infection from eyes to periocular tissues via zosteriform spread (28). Recently, lead compounds directed against the helicase-primase enzyme of HSV-1 were described, and these compounds were reported to be more effective than established nucleoside analogs in the treatment of acute infection (8, 14). Potentially, further development of these and other new drugs for HSV-1 could be facilitated greatly by bioluminescence imaging technology, because serial studies of drug pharmacokinetics and overall efficacy could be determined in the same cohort of mice.

Although we anticipate that bioluminescence imaging will enhance research into pathogenesis of HSV-1 in vivo, this imaging modality will not completely replace conventional assays. Because the spatial resolution of bioluminescence imaging is ca. 2 to 3 mm, the technique cannot differentiate between sources of light emanating from sites that are in close anatomic proximity. Thus, imaging did not detect the established decrease in FL activity in eye tissue and subsequent increase in reporter function in periocular tissues that occurs during acute infection and zosteriform spread of virus (28). Bioluminescence imaging currently produces only two-dimensional data, so light detected by the camera is a summation of all photons produced in a given plane. As a result, we were unable to distinguish light produced by KOS/Dlux/oriL in trigeminal ganglia from overlying periocular tissues in the intact mouse. Because light is attenuated by ca. 10-fold per centimeter of tissue (5), most bioluminescence in the images likely originated in periocular skin rather than in trigeminal ganglia. Potentially, three-dimensional localization of photons will be improved by the development of bioluminescence imaging systems that allow cross-sectional imaging. Additionally, light emission occasionally may be seen from nonphysiologic sites, such as the

nose cone used for anesthesia. However, these spurious sources of light emission usually can be identified as reflected light or background noise of the imaging system at low levels of FL activity.

Bioluminescence imaging of RL has been reported previously after systemic delivery of coelenterazine (2), but we were unable to detect the activity of this reporter protein in the footpads or eyes of mice infected with KOS/Dlux/oriL. However, RL could be imaged after direct application of coelenterazine to the cornea, demonstrating that the pharmacokinetics and bioavailability of substrate after systemic administration limited the in vivo bioluminescent reaction. This limitation potentially could be overcome by increasing the dose of coelenterazine, thus enabling imaging of two different luciferase reporters in vivo. From a practical perspective, the high cost of coelenterazine currently precludes significant increases in amount of administered substrate.

In summary, our data validate bioluminescence imaging for monitoring HSV-1 infection in vivo and demonstrate significant advantages of bioluminescence imaging over conventional methods used to investigate viruses in mouse models. Noninvasive imaging allows the same group of animals to be studied over time, which reduces the number of animals used in experiments. By enabling serial studies on the same animal, this imaging technique can overcome animal-to-animal variations in experimental data. Potentially, noninvasive imaging could facilitate the discovery and development of new antiviral drugs. In addition, immune cell trafficking during the host response to HSV-1 infection could be monitored by stably expressing FL in defined populations of host cells (7). However, limitations of spatial resolution may hinder selected applications of this imaging technique. Overall, we anticipate that bioluminescence imaging will become an important technology for investigating pathogenesis of HSV-1 and other viruses.

ACKNOWLEDGMENTS

We thank Kathryn Luker for helpful discussions.

This study was funded by NIH grants RO1 EY09083 to D.A.L., P20 CA86251 and P50 CA94056 to D.P.-W., and P30 EY02687 to the Department of Ophthalmology and Visual Sciences. Support from the McDonnell Foundation to G.D.L. and from Research to Prevent Blindness to the Department of Ophthalmology and Visual Sciences and a Robert E. McCormick Scholarship to D.A.L. are gratefully acknowledged.

REFERENCES

1. **Benaron, D., P. Contag, and C. Contag.** 1997. Imaging brain structure and function, infection and gene expression in the body using light. Philos. Trans. R. Soc. Lond. B Biol. Sci. **352:**755–761.
2. **Bhaumik, S., and S. Gambhir.** 2001. Optical imaging of *Renilla* luciferase reporter gene expression in living mice. Proc. Natl. Acad. Sci. USA **99:**377–392.
3. **Blyth, W., D. Harbour, and T. Hill.** 1984. Pathogenesis of zosteriform spread of herpes simplex virus in the mouse. J. Gen. Virol. **65:**1477–1486.
4. **Coen, D., M. Kosz-Vnenchak, J. Jacobson, D. Leib, C. Bogard, P. Schaffer, K. Tyler, and D. Knipe.** 1989. Thymidine kinase negative herpesvirus mutants establish latency in mouse trigeminal ganglia, but do not reactivate. Proc. Natl. Acad. Sci. USA **86:**4736–4740.
5. **Contag, C., P. Contag, J. Mullins, S. Spilman, D. Stevenson, and D. Benaron.** 1995. Photonic detection of bacterial pathogens in living hosts. Mol. Microbiol. **18:**593–603.
6. **Contag, C., S. Spilman, P. Contag, M. Oshiro, B. Eames, P. Dennery, D. Stevenson, and D. Benaron.** 1997. Visualizing gene expression in living mammals using a bioluminescent reporter. Photochem. Photobiol. **66:**523–531.
7. **Costa, G., M. Sandora, A. Nakajima, E. Nguyen, C. Taylor-Edwards, A. Slavin, C. Contag, C. Fathman, and J. Benson.** 2001. Adoptive immunotherapy of experimental autoimmune encephalomyelitis via T cell delivery of the IL-12 p40 subunit. J. Immunol. **167:**2379–2387.
8. **Crute, J., C. Grygon, K. Hargrave, B. Simoneau, A. Faucher, G. Bolger, P. Kibler, M. Liuzzi, and M. Cordingley.** 2002. Herpes simplex virus helicase-primase inhibitors are active in animal models of human disease. Nat. Med. **8:**386–391.
9. **Dyson, H., C. Shimeld, T. Hill, W. Blyth, and D. Easty.** 1987. Spread of herpes simplex virus within ocular nerves of the mouse: demonstration of viral antigen in whole mounts of eye tissue. J. Gen. Virol. **68:**2989–2995.
10. **Feldman, L., A. Ellison, C. Voytek, L. Yang, P. Krause, and T. Margolis.** 2002. Spontaneous molecular reactivation of herpes simplex virus type 1 latency in mice. Proc. Natl. Acad. Sci. USA **99:**978–983.
11. **Francis, K., D. Joh, C. Bellinger-Kawahara, M. Hawkinson, T. Purchio, and P. Contag.** 2000. Monitoring bioluminescent *Staphylococcus aureus* infections in live mice using a novel *luxABCDE* construct. Infect. Immun. **68:**3594–3600.
12. **Francis, K., J. Yu, C. Bellinger-Kawahara, D. Joh, M. Hawkinson, G. Xiao, T. Purchio, M. Cararon, M. Lipsitch, and P. Contag.** 2001. Visualizing pneumococcal infections in the lungs of live mice using bioluminescent *Streptococcus pneumonia* transformed with a novel gram-positive *lux* transposon. Infect. Immun. **69:**3350–3358.
13. **Glantz, S. A.** 1987. Primer of biostatistics, 2nd ed. McGraw-Hill, Inc., New York, N.Y.
14. **Kleymann, G., R. Fisher, U. Betz, M. Hendrix, W. Bender, U. Schneider, G. Handke, P. Eckenberg, G. Hewlett, V. Pevzner, J. Baumeister, O. Weber, K. Henninger, J. Keldenich, A. Jensen, J. Kolb, U. Bach, A. Popp, J. Maben, I. Frappa, D. Haebich, O. Lockhoff, and H. Rubsamen-Waigman.** 2002. New helicase-primase inhibitors as drug candidates for the treatment of herpes simplex disease. Nat. Med. **8:**392–398.
15. **Labetoulle, M., P. Kucera, G. Ugolini, F. Lafay, E. Frau, H. Offret, and A. Flamand.** 2000. Neuronal propagation of HSV1 from the oral mucosa to the eye. Investig. Ophthalmol. Vis. Sci. **41:**2600–2606.
16. **Lee, L., and P. Schaffer.** 1998. A virus with a mutation in the ICP4-binding site in the L/ST promoter of herpes simplex virus type 1, but not a virus with a mutation in open reading frame P, exhibits cell-type-specific expression of $\gamma_1$34.5 transcripts and latency-associated transcripts. J. Virol. **72:**4250–4264.
17. **Leib, D., D. Coen, C. Bogard, K. Hicks, D. Yager, D. Knipe, K. Tyler, and P. Schaffer.** 1989. Immediate-early regulatory gene mutants define different stages in the establishment and reactivation of herpes simplex virus latency. J. Virol. **63:**759–768.
18. **Leib, D., T. Harrison, K. Laslo, M. Machalak, N. Moorman, and H. Virgin.** 1999. Interferons regulate the phenotype of wild-type and mutant herpes simplex viruses in vivo. J. Exp. Med. **189:**663–672.
19. **Leib, D., M. Machalek, B. Williams, R. Silverman, and H. Virgin.** 2000. Specific phenotypic restoration of an attenuated virus by knockout of a host resistance gene. Proc. Natl. Acad. Sci. USA **97:**6097–6101.
20. **Lipshutz, G., C. Gruber, Y. Cao, J. Hardy, C. Contag, and K. Gaensler.** 2001. In utero delivery of adeno-associated viral vectors: intraperitoneal gene transfer produces long-term expression. Mol. Ther. **3:**284–292.
21. **Lorenz, W., M. Ro, M. Longiaru, and M. Cormier.** 1991. Isolation and expression of a cDNA encoding *Renilla* reniformis luciferase. Proc. Natl. Acad. Sci. USA **88:**4438–4442.
22. **O'Connell-Rodwell, C., S. Burns, M. Bachmann, and C. Contag.** 2002. Bioluminescent indicators for in vivo measurements of gene expression. Trends Biotechnol. **20:**S19–S23.
23. **Preston, C.** 2000. Repression of viral transcription during herpes simplex virus latency. J. Gen. Virol. **81:**1–19.
24. **Pyles, R., N. Sawtell, and R. Thompson.** 1992. Herpes simplex virus type 1 dUTPase mutants are attenuated for neurovirulence, neuroinvasiveness, and reactivation from latency. J. Virol. **66:**6706–6713.
25. **Rader, K., C. Ackland-Berglund, J. Miller, J. Pepose, and D. Leib.** 1993. In vivo characterization of site-directed mutations in the promoter of the herpes simplex virus type 1 latency-associated transcripts. J. Gen. Virol. **74:**1859–1869.
26. **Sadikot, R., E. Jansen, T. Blackwell, O. Zoia, F. Yull, J. Christman, and T. Blackwell.** 2001. High-dose dexamethasone accentuates nuclear factor-κβ activation in endotoxin-treated mice. Am. J. Respir. Crit. Care Med. **164:**873–878.
27. **Summers, B., and D. Leib.** 2002. Herpes simplex virus type 1 origins of DNA replication play no role in the regulation of flanking promoters. J. Virol. **76:**7020–7029.
28. **Summers, B., T. Margolis, and D. Leib.** 2001. Herpes simplex virus type 1 corneal infection results in periocular disease by zosteriform spread. J. Virol. **75:**5069–5075.
29. **Sweeney, T., V. Mailander, A. Tucker, A. Olomu, W. Zhang, Y. Cao, R. Negrin, and C. Contag.** 1999. Visualizing the kinetics of tumor-cell clearance in living animals. Proc. Natl. Acad. Sci. USA **96:**12044–12046.
30. **Taus, N., and W. Mitchell.** 2001. The transgenic ICP4 promoter is activated in schwann cells in trigeminal ganglia of mice latently infected with herpes simplex virus type 1. J. Virol. **75:**10401–10408.
31. **Thackray, A., and H. Field.** 2000. The effects of antiviral therapy on the distribution of herpes simplex virus type 1 to ganglionic neurons and its

consequences during, immediately following and several months after treatment. J. Gen. Virol. **81:**2585–2596.
32. **Tran, R., P. Lieu, S. Aguilar, E. Wagner, and D. Bloom.** 2002. Altering the expression kinetics of VP5 results in altered virulence and pathogenesis of herpes simplex virus type 1 in mice. J. Virol. **76:**2199–2205.
33. **Whitley, R.** 1996. Herpes simplex viruses, p. 2297–2342. *In* B. Fields, D. Knipe, P. M. Howley, et al. (ed.), Fields virology, 3rd ed. Lippincott-Raven Publishers, Philadelphia, Pa.
34. **Wu, J., G. Sundaresan, M. Iyer, and S. Gambhir.** 2001. Noninvasive optical imaging of firefly luciferase reporter gene expression in skeletal muscles of living mice. Mol. Ther. **4:**297–306.
35. **Yamada, Y., H. Kimura, T. Morishima, T. Daikoku, K. Maeno, and Y. Nishiyama.** 1991. The pathogenicity of ribonucleotide reductase-null mutants of herpes simplex virus type 1 in mice. J. Infect. Dis. **164:**1091–1097.